InP Photonic Integrated Circuits

Radhakrishnan Nagarajan, *Fellow, IEEE*, Masaki Kato, *Member, IEEE*, Jacco Pleumeekers, Peter Evans, Scott Corzine, Sheila Hurtt, Andrew Dentai, *Fellow, IEEE*, Sanjeev Murthy, Mark Missey, Ranjani Muthiah, *Member, IEEE*, Randal A. Salvatore, *Member, IEEE*, Charles Joyner, Richard Schneider, Jr., Mehrdad Ziari, *Member, IEEE*, Fred Kish, *Senior Member, IEEE*, and David Welch, *Fellow, IEEE*

(Invited Paper)

***Abstract*—InP is an ideal integration platform for optical generation, switching, and detection components operating in the range of 1.3–1.6 μm wavelength, which is preferred for data transmission in the most prevalent silica-based optical fiber. We review the current state of the art in advanced InP photonic ICs.**

***Index Terms*—Monolithic InP integration, multichannel dense wavelength-division-multiplexed (DWDM) transmitter and receiver, photonic IC.**

I. Introduction

PHOTONIC integration has a very rich and active research history dating back to the late 1960s [1]. This area of development that started with the integration of a handful of devices saw the first commercial deployment of large-scale photonic ICs (LS-PICs), with over 50 discrete components monolithically integrated onto to a single InP substrate, only five years ago. Experimentally, monolithically integrated devices on InP with well over 200 components have been demonstrated to date.

Although there are many metrics, Fig. 1 graphically shows the progression of PIC complexity, as measured in the number of integrated components on a single InP substrate, with time. The details of the devices presented in Fig. 1 are covered in [2]–[21] (the references are next to the devices in Fig. 1).

For the first decade or so after, with the demonstration of the continuous-wave (CW) laser in the GaAs system, InP lasers started to mature. In the mid 1980s, there was active work in the area of optoelectronic ICs (OEICs), where the integration of electronic devices like HBT and FET with laser diodes and photodetectors (PDs) was pursued. In the late 1980s, three section-tunable distributed Bragg reflector (DBR) lasers were introduced. This was also when electroabsorption modulators (EAMs) integrated with DFB lasers were demonstrated. The trend continued with more complicated (four and five section) tunable laser sources, which were also integrated with an EAM or a semiconductor optical amplifier (SOA). The next step was the demonstration of the arrayed waveguide grating (AWG) or phased array (PHASAR) router integrated with PDs for multichannel receivers or with gain regions and EAM for multifrequency lasers and multichannel modulated sources. One of the most complex PICs reported in the last century was a four-channel optical cross-connect integrating two AWGs with 16 Mach–Zehnder interferometer (MZI) switches. At this stage, the most sophisticated laboratory devices still had component counts below 20, while those in the field had component counts of about four.

The trend in low-level photonic integration continued into the 21st century with one of the larger chips reported, being a 32-channel wavelength-division-multiplexed (WDM) channel selector. First steps toward a larger integrated chip were reported in 2003. ThreeFive Photonics reported a 40-channel WDM monitor chip, integrating nine AWGs with 40 detectors. MetroPhotonics reported a 44-channel power monitor based on an echelle grating demultiplexer. The commercial development of both chips was subsequently discontinued. The first successful attempt, at a commercial large-scale photonic-integrated chip, was made in 2004 when Infinera introduced a 10-channel transmitter, with each channel operating at 10 Gb/s. This device, with an integration count in excess of 50 individual components, was the first LS-PIC device deployed in the field to carry live network traffic. This was quickly followed, in 2006, by a 40-channel monolithic InP transmitter, each channel operating at 40 Gb/s, with a total component count larger than 240, aggregate data rate of 1.6 Tb/s, and a complementary 40-channel receiver PIC. As a further step in complexity, the 40-channel receiver PIC also had an integrated, polarization independent (PI), multichannel SOA at the input. This level of complexity is still the benchmark for monolithic integration in InP. Recently, in 2009, University of California, Santa Barbara (UCSB), reported an 8×8 monolithic tunable router with component count of about 200.

The Infinera large-scale PIC platform has not only been shown to be highly scalable, but also highly manufacturable and highly reliable [22]–[24]. At the time of writing, the 10-channel variant of the PIC has accumulated over 200 million device-pair hours operating in the field without failure.

In this paper, we will review details of the most advanced InP PICs that we have built and reported to date. After a brief overview of PIC fabrication techniques in Section II–IV describe the PICs we designed for amplitude-modulated OOK systems.

Manuscript received September 11, 2009; revised November 19, 2009; accepted November 24, 2009. Date of publication January 26, 2010; date of current version October 6, 2010.

The authors are with the Infinera Corporation, 1322 Bordeaux Drive, Sunnyvale, CA 94089 USA (e-mail: rnagarajan@infinera.com; mkato@infinera.com; jpleumeekers@infinera.com; pevans@infinera.com; scorzine@infinera.com; shurtt@infinera.com; adentai@infinera.com; smurthy@infinera.com; mmissey@infinera.com; rmuthiah@infinera.com; rsalvatore@infinera.com; cjoyner@infinera.com; rschneider@infinera.com; mziari@infinera.com; fkish@infinera.com; dwelch@infinera.com).

Color versions of one or more of the figures in this paper are available online at http://ieeexplore.ieee.org.

Digital Object Identifier 10.1109/JSTQE.2009.2037828

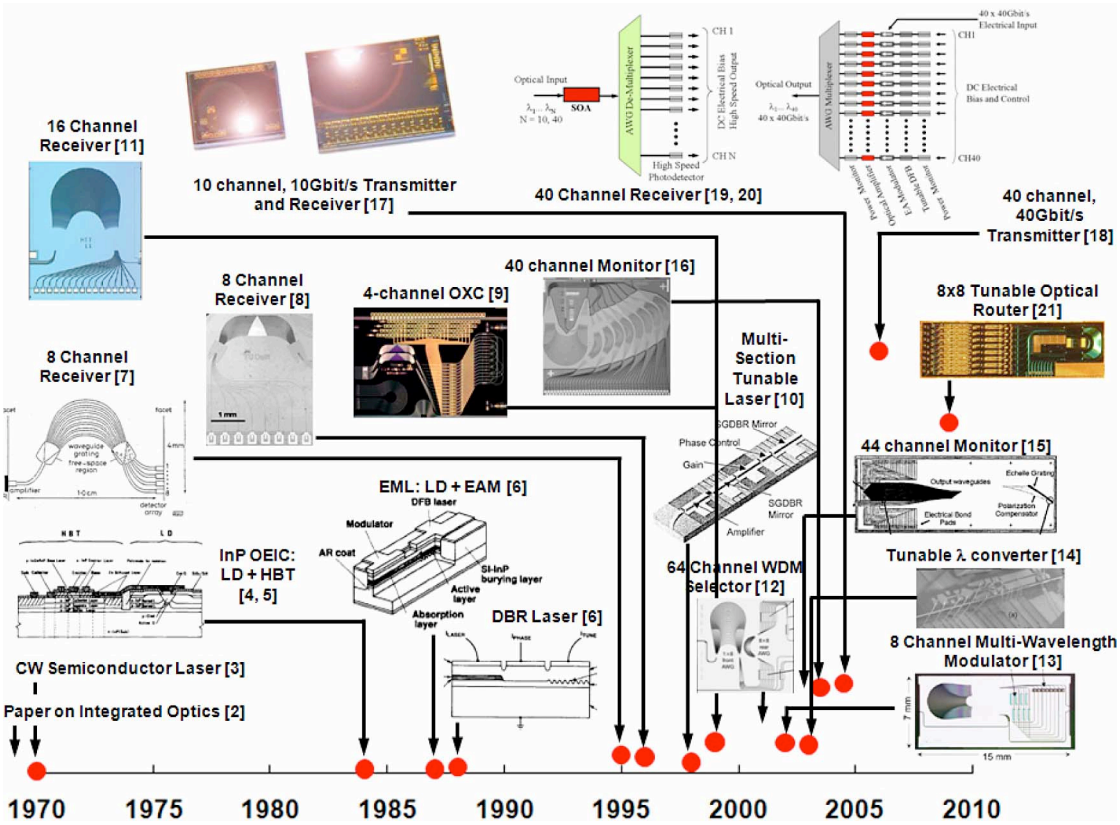

Fig. 1. Historical trend and timeline for monolithic, photonic integration on InP (Refs are next to the description of the devices in the figure). We have not included vertical cavity InP devices. The vertical scale is linear, and the red filled circles start at 1 and go to 240. The trend shows an exponential growth in PIC complexity in recent years. Unlike Si ICs where the transistor count is an universal metric, there is no unique benchmark for complexity in photonic integration. For this exercise, we have counted a functional unit (which may be a combination of other optical elements) as a device. For example, an MZI is counted as 1 and not as 3. Likewise, an AWG is counted as 1, irrespective of the fraction of the PIC real estate it occupies.

In Section V, we describe our work in the area of PICs designed for phase-modulated QPSK systems.

II. PIC Fabrication

A. General Overview

Components like lasers, modulators (electroabsorption or interferometric), PDs, optical amplifiers, optical multiplexers, and low-loss waveguides need to be integrated on a common platform to realize the complicated chips that have been demonstrated to date. These components have very different epitaxial requirements. The integration process needs to accommodate these without sacrificing the performance of the PIC. We will only briefly review some of the common techniques that have been used. Methods range from the use of multiple epitaxial steps to ones that accomplish everything with a single epitaxial step.

The epitaxial layers are normally grown by metal–organic chemical vapor deposition (MOCVD) on an InP substrate. The active regions are typically composed of the InGaAsP or the AlGaInAs quaternaries. The different active regions are then integrated using one of the three common techniques. We have used a conventional growth–etch–regrowth technique to fabricate our PICs [17]. This is the most versatile technique, but requires very good manufacturing control of the fabrication and epitaxial processes.

Another technique to get active regions of various bandgaps is to use quantum-well intermixing (QWI) to selectively shift the bandgap of the as-grown epitaxial layers [25]. The group at UCSB has successfully used an impurity-free QWI process, followed by a blanket regrowth to fabricate their PICs [21].

OneChip Photonics uses a process called multiguide vertical integration (MGVI) to fabricate their PICs [26]. Here, the various epitaxial layers are grown vertically stacked on top of one another in the ascending order of their core layer bandgap wavelengths. A series of mode adaptors are then used to couple light in and out of the various functional elements that have been stacked vertically. The complete PIC design is achieved with a single epitaxial step. This requires a careful design of the epitaxial stack and the various mode transformers to achieve the desired device performance.

A common device design used to build these PICs is the ridge waveguide structure [21], [26]. This is a simpler process where the ridge forming the device is either air clad or may be passivated using a dielectric layer. The group at the University of California, Davis, has used a buried waveguide process and has demonstrated PICs using Fe InP regrowth to planarize and passivate the waveguides [27].

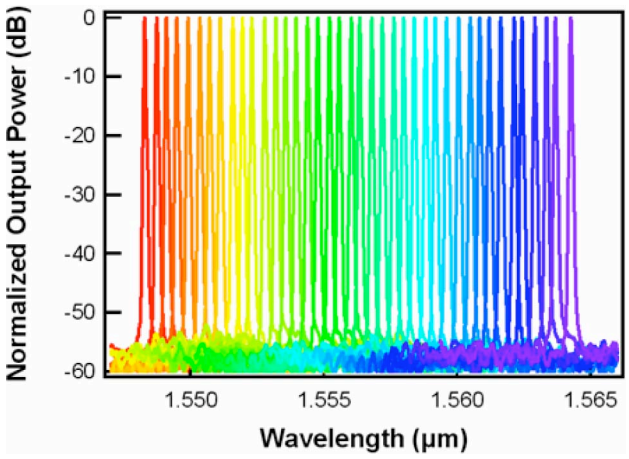

Fig. 2. Normalized output optical spectrum of the 40-channel PIC.

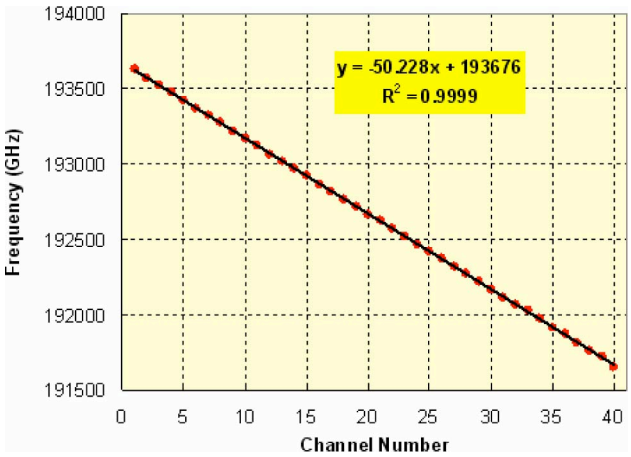

Fig. 3. Distribution of the channel peak frequencies.

III. 40-Channel Amplitude-Modulated Transmitter PIC

A. Device Details

The architecture of the 40-channel transmitter PIC is shown in the top right-hand corner of Fig. 1. Each individual transmit channel consists of a tunable DFB with a back-facet power monitor, an EAM, a SOA, and a front-facet power monitor. The 40 different wavelength channels are then combined using the AWG multiplexer, resulting in a single optical output.

B. DC and RF Performance

The normalized, fiber-coupled, output power spectrum of the 40-channel PIC is shown in Fig. 2. The temperature of the PIC is stabilized at 25 °C. The per-channel SOA is used to level the output power from the individual channels.

The output frequency, as a function of channel number, is shown in Fig. 3. The linear fit to the data shows an average channel spacing of 50 GHz between the channels. The total span of the 40 channels is about 16 nm, and covers half of the traditional C band in the transmission fiber.

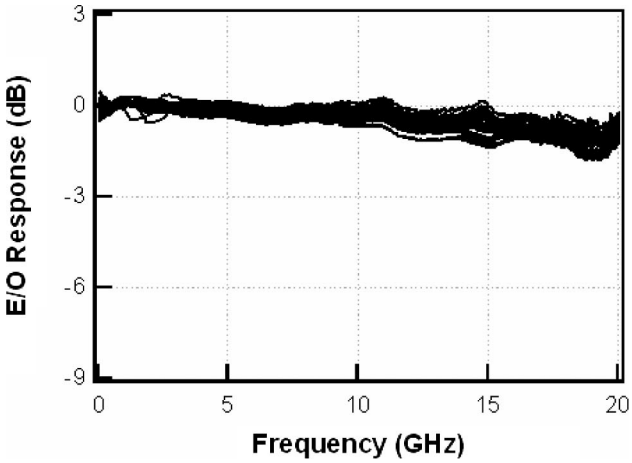

Fig. 4. Normalized electrical S21 response of all 40 EAM's on the PIC.

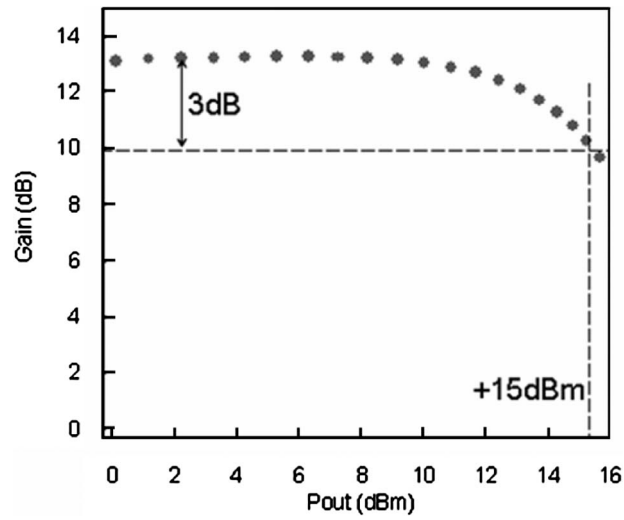

Fig. 5. Integrated transmitter SOA gain characteristics.

Fig. 4 shows the normalized electrical S21 curves of the EAM measured at a nominal reverse bias of 2 V using an Agilent 8703B lightwave component analyzer. Although the bandwidth of the electrooptic measurement setup is limited to 20 GHz, point at which the individual responses uniformly drop by about 1.5 dB, the extrapolated response shows that the devices have sufficient bandwidth for modulation at 40 Gb/s.

The SOA was characterized using the photocurrent from the reverse-biased detectors integrated on the PIC, with light injected in the reverse direction into the PIC from an external tunable laser. Fig. 5 shows that the SOA has a gain of 13 dB and an output saturation power (P_{sat}) of 15 dBm. The SOA's (one per wavelength path) do not lead to any Q performance impairments and have very good long-term reliability [28]. Transmitter PICs with SOA's are currently deployed in the field carrying live traffic.

A potential impairment for simultaneous operation of multiple channels on a single substrate PIC is signal crosstalk. This is especially important for channel counts as high as 40. There are two varieties of crosstalk: optical and electrical.

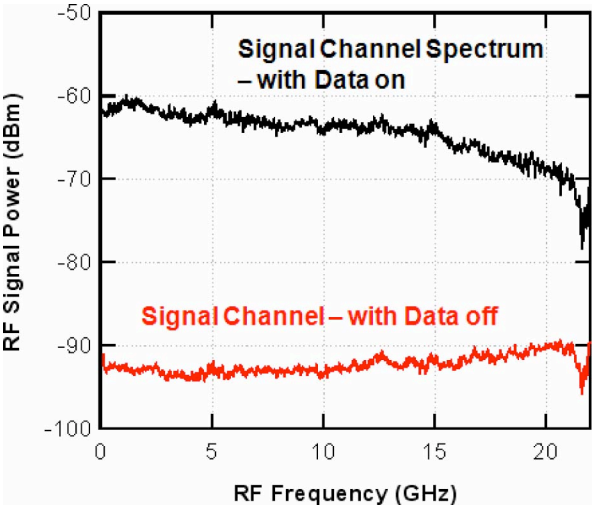

Fig. 6. RF spectrum from the channel under test with and without the 40-Gb/s data being applied.

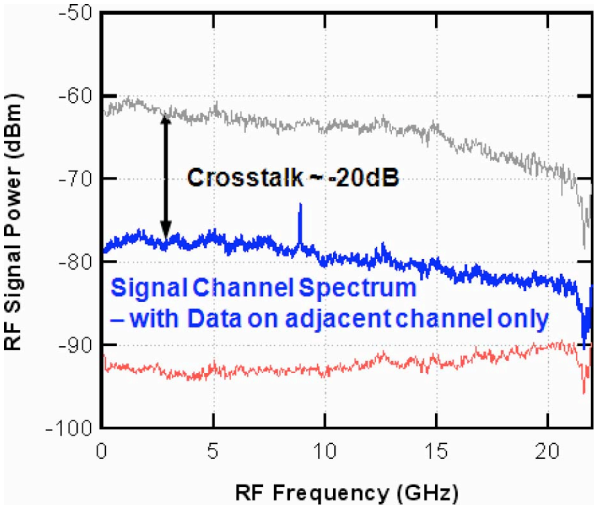

Fig. 7. RF spectrum from the channel under test with the 40 Gb/s data being applied to the adjacent channel. The "lightened" red and black traces are the ones from Fig. 6, shown here for reference.

Optical crosstalk is not a problem at the transmitter. Since all the channels are eventually combined into one single output, the individual paths traversed by the wavelengths on the PIC are irrelevant for sufficiently spaced waveguide layouts. The only remaining concern is the eye distortion due to filtering by the AWG. For this PIC, the AWG optical passband shape was a Gaussian, and the nominal 3-dB bandwidth was 90 GHz. This is sufficiently wide to prevent any distortion due to filtering at the AWG.

Electrical crosstalk, which is potentially important, occurs when the signal being applied to one wavelength (channel) appears as a part of the output from the adjacent wavelength (channel). We measured the electrical crosstalk, using the Agilent 71400C lightwave signal analyzer, while the 40 Gb/s data were being applied to the adjacent channel. Fig. 6 shows the RF spectrum of the channel under test, with and without the 40 Gb/s data being applied.

Fig. 7 shows the RF spectrum from the same channel when the signal is applied to the adjacent channel. The adjacent channel electrical crosstalk is nominally 20 dB below the signal channel power level indicating that electrical crosstalk may not be a significant impairment. Thus, the 40-channel PIC should be capable of simultaneous operation at 1.6 Tb/s without significant crosstalk impairments.

Fig. 8 shows the output eye diagram for all the 40 channels operating at 40 Gb/s from the PIC measured using an Agilent 86100A digital communication analyzer (DCA) with 30-GHz optical plug-in (86109A). Bandwidth limitations in the plug-in result in some filtering and transmitter eye closure. The EAMs of the PIC were individually modulated with a (2^7-1), 40-Gb/s nonreturn-to-zero (NRZ) data stream from a pseudorandom bit sequence (PRBS) generator. The eye diagrams are very uniform over all 40 channels, demonstrating a robust design and a high degree of control in manufacturing. The extinction ratio for all channels is the range of 6–8 dB. The EAM was driven using a broadband driver amplifier with a 2.5–3.0 V voltage swing. The average EAM bias voltage was -1.7 V.

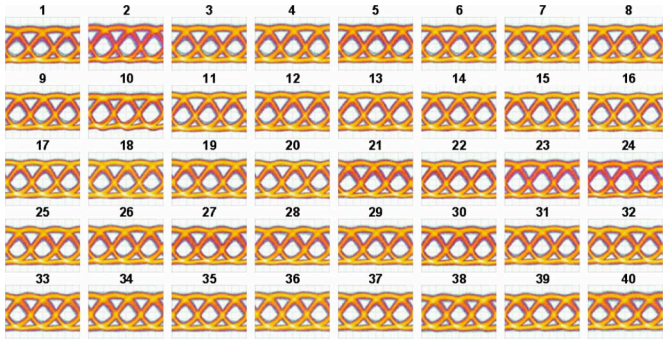

Fig. 8. 40-Gb/s NRZ eye diagrams for all 40 channels of the transmitter PIC.

IV. 40-Channel Amplitude-Modulated Receiver PIC

A. Device Details

Fig. 1 (top right corner, to the left of 40-channel transmitter PIC) shows the architecture of the receiver PIC. There is a wide bandwidth, multichannel SOA at the input. The input channels, up to a maximum of 40, are demultiplexed using an AWG router. The demultiplexed channels are terminated in an array of high speed, waveguide PDs. The SOA and AWG are designed to be PI.

Fig. 9 shows the input slab of the AWG demultiplexer. At the facet, the light can either be coupled into a SOA channel or a reference channel that bypasses the SOA. This design feature allows us to characterize the receiver in the absence of the SOA and also to measure the net gain of the SOA. This is critical for the characterization of the SOA, on-PIC, without any elaborate hardware setup.

The basic principle of making a PI SOA is to balance the polarization properties of the waveguide structure, which tends to favor the TE polarization, with that of the gain medium, which is designed to have net tensile strain, and hence, favor the TM polarization. This principle is discussed extensively in the literature [29]–[38]. This balance equation can be written as

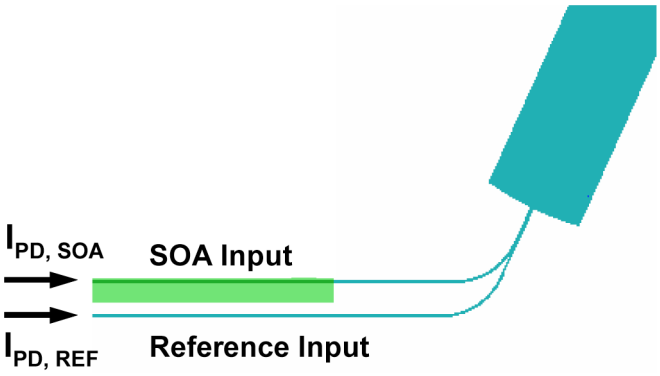

Fig. 9. AWG has two inputs; one is with the SOA, and the other is the reference channel, without the SOA.

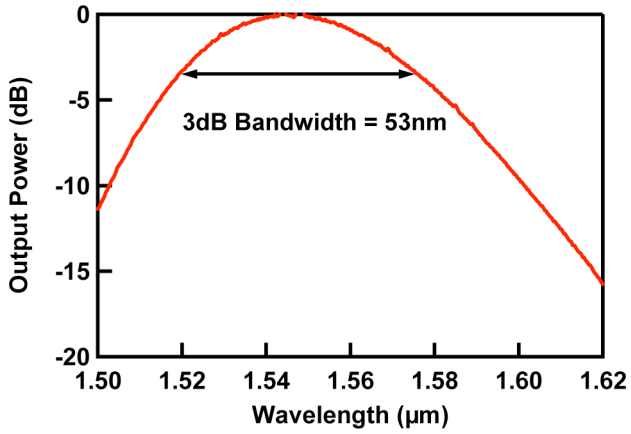

Fig. 10. Normalized ASE spectrum of the SOA.

follows:

$$\Gamma_{\mathrm{TE}} g_{\mathrm{TE}} = \Gamma_{\mathrm{TM}} g_{\mathrm{TM}}$$

where Γ_{TE} and Γ_{TM} are the TE and TM optical mode overlap factors, respectively, and g_{TE} and g_{TM} are the TE and TM material gains of the active region, respectively.

In the case of quantum-well active region, a combination of compressive (only TE emission) and tensile (mainly TM and some TE emission) strain wells/barriers is used to obtain an active region with PI gain [30], [31]. In the case of bulk active region, which is a simpler epitaxial structure, it is just grown with a net tensile strain.

The mode overlap factor is also influenced by the choice of the device structure, a buried heterostructure [33]–[35], [37], or a ridge waveguide [36]. In addition to these, there are numerous manufacturing tolerances that affect the difference in the gain between the TE and TM modes as well [38]. This gain difference is called the polarization-dependent gain (PDG).

PDG is also a function of SOA bias current. Unlike a semiconductor laser, the carrier density in the SOA continues to increase with bias current. This changes the bandfilling in the active region, and hence, the ratio of TE to TM gains. Operating bias current, from the perspective of the total SOA power consumption, is an important device design parameter.

There are two competing criteria in the design of a SOA: gain (G) and saturated output power (P_{sat}). The first design parameter for which a tradeoff is needed is the mode overlap factor that is inversely related to the saturation output power. Gain on the other hand is linearly related to the mode overlap factor.

High-gain devices require a larger optical mode overlap with the active region, whereas the reverse is true for high P_{sat} devices [35], [37]. Likewise, thicker active regions have higher gain and thinner active regions have higher P_{sat} [33], [37]

$$P_{\mathrm{sat,TE/TM}} \propto 1/\Gamma_{\mathrm{TE/TM}}$$
$$G_{\mathrm{TE/TM}} \propto \Gamma_{\mathrm{TE/TM}}.$$

The third competing design parameter is the cavity length. Again a similar tradeoff holds, longer cavities have higher gain and lower P_{sat}.

Given the number of performance tradeoffs, it is difficult to pinpoint any one epitaxial design that would be successful for all the specifications. For most relevant applications, bulk active regions with a tensile strain in the range of 0.5%–2.5% and thicknesses in the range of 500–2500Å are suitable. It is important to note that these design parameters are inversely related to one another; the thicker active regions required for higher gain in shorter SOA lengths, also require lower strains for polarization independence.

In the case of quantum-well SOA designs, there is a range of options from incorporating the strain just in the wells to strain-compensated structures. Quantum well and barrier thicknesses can also be tailored. Tensile strains in range of 0.2%–1.7%, with appropriate strain compensation or tailoring of quantum well and barrier thicknesses, are suitable.

There are several excellent references [11], [39]–[43] and commercial design tools [44] available for AWG design (InP or otherwise). Low-loss and PI design methodologies are also discussed in these references. We will not review these in detail here.

B. Integrated SOA DC Performance

Fig. 10 shows the normalized amplified spontaneous emission (ASE) spectrum or equivalently the normalized extent of the gain spectrum of the SOA. The spectrum was measured at a bias current of 250 mA, and the SOA has a 3-dB optical bandwidth of 53 nm with the center wavelength at about 1550 nm. The ASE spectrum from the SOA was measured in the reverse direction (output from the facet) using an optical spectrum analyzer (OSA) with a circulator at the input.

Fig. 11 shows the normalized amplified response of a 10-channel receiver PIC at 200-GHz channel spacing. For this measurement, the temperature of the PIC was 20 °C.

The transmission spectrum of the PIC was measured for the polarizations with maximum and minimum transmissions (bold and dashed lines) to quantify the PDG and polarization-dependent wavelength shift (PDWS). Unlike PDG, PDWS is peculiar to a multichannel receiver integrated with a wavelength sensitive demultiplexer like an AWG. PDWS is the result of

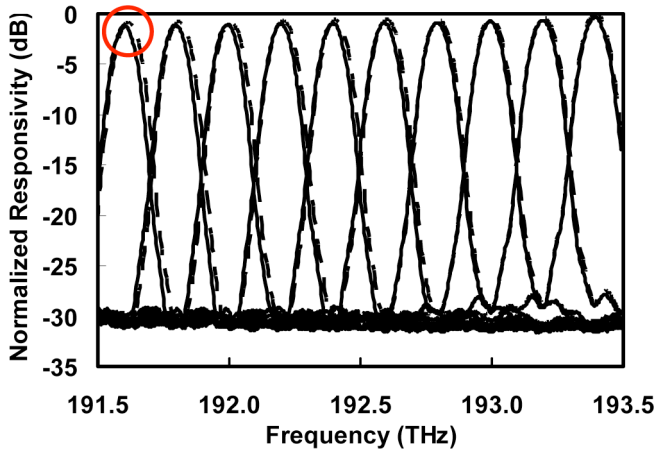

Fig. 11. Amplified transmission spectrum of a 10-channel receiver PIC.

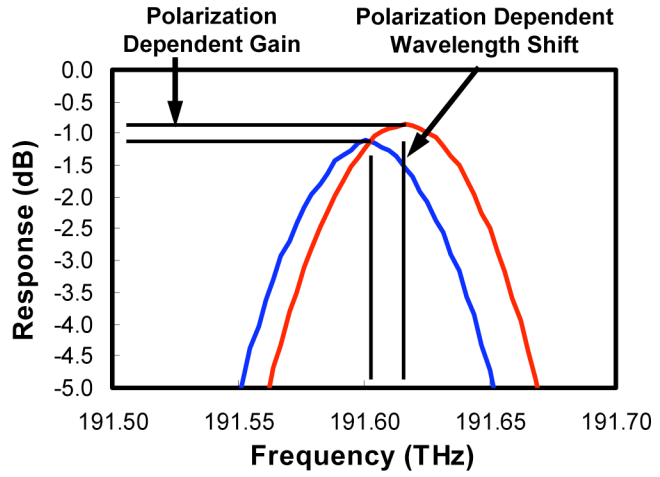

Fig. 12. Close-up of the circled part of the spectrum in Fig. 11 indicating the details of the PDG and PDWS components.

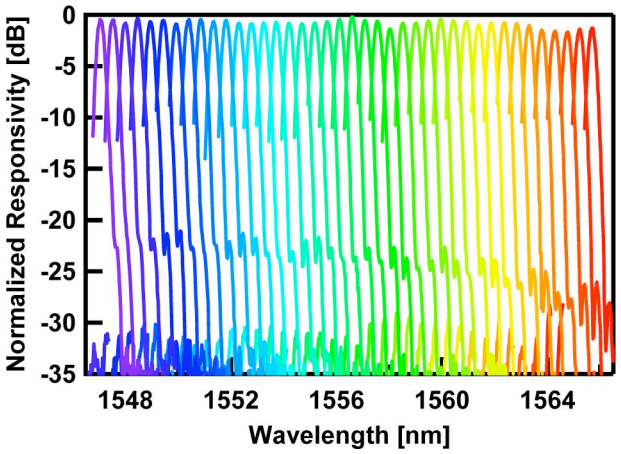

Fig. 13. Amplified transmission spectrum of a 40-channel receiver PIC.

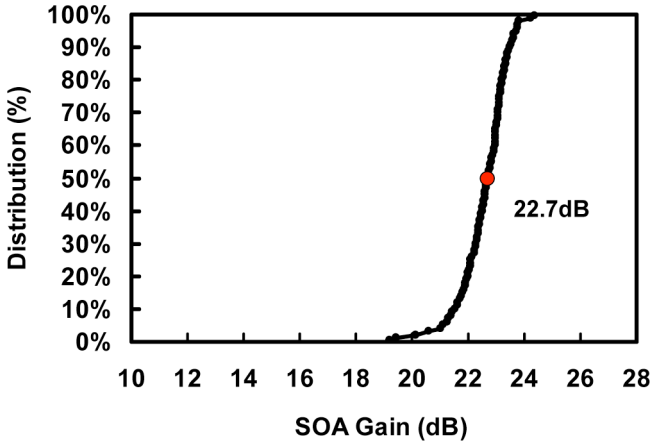

Fig. 14. SOA gain distribution for 300 channels.

the demultiplexer having slightly different mode indexes, in the grating arms, for the propagation of the two orthogonal polarizations.

Fig. 12 shows the worst-case PDWS and PDG for the PIC response shown in Fig. 11 (Fig. 12 is the enlargement of the area enclosed in a circle in Fig. 11). The effective PDG of the PIC has contributions from both the PDG of the SOA and polarization-dependent loss (PDL) of the AWG.

Fig. 13 shows the transmission spectrum of a 40-channel receiver PIC. The channel spacing for the 40-channel receiver is 50 GHz, and the PDWS becomes a very stringent criterion for the design of the AWG at smaller channel spacings. The power flatness for the whole PIC is less than ± 0.75 dB over all 40 channels. The total spectral width of the 40-channel device at 50-GHz spacing is equivalent to the 10-channel device with 200-GHz spacing. Hence, the same SOA design is applied to both cases, with appropriate scaling in the per-channel optical power to maintain the same total output power.

The net gain of the SOA (and its spectral and polarization dependence) is computed first by measuring the response of the SOA input and correcting it with the response measured at the reference input (see Fig. 9). Using the ratio of the photocurrents, when the light is coupled to the SOA channel ($I_{\mathrm{PD,SOA}}$), to the photocurrent when it is coupled to the reference channel ($I_{\mathrm{PD,REF}}$), we can calculate the net gain of the SOA. The differences in fiber-coupling efficiency between the reference and SOA inputs at the facet may provide some variability in this measurement.

Fig. 14 shows the gain, and Fig. 15 shows the PDG distribution for the 10-channel receiver PIC (SOA and AWG combined). The median gain is 22.7 dB. The total variability in gain (95%–5%) over 300 channels is about 2.5 dB. This distribution includes the variation of the SOA gain spectrum, the variation in the AWG response, and the run-to-run manufacturing variation for all the channels in the PIC. The maximum PDG over the same number of devices is less then 0.8 dB (95% point of the distribution). Although, we investigated SOA's of various lengths, the data in Figs. 14 and 15 are for a 900-μm-long cavity. The SOA bias current is 250 mA.

Fig. 16 shows the gain saturation behavior of the SOA as a function of output power. The -3 dB saturation output power (P_{sat}) is 16 dBm. This P_{sat}, obtained here at a lower pump current, is comparable to the best values published for a standalone PI SOA [37].

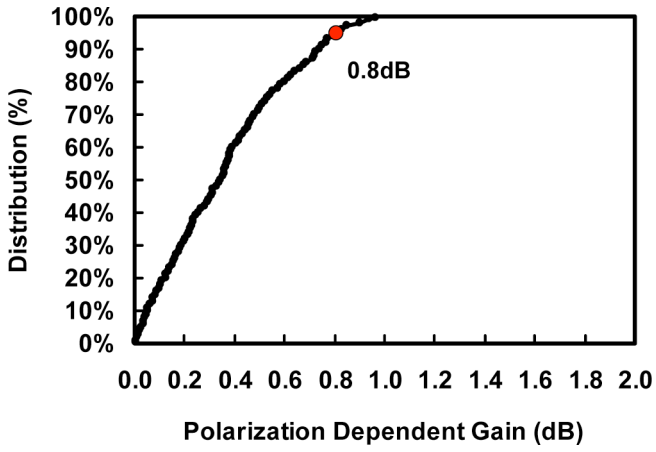

Fig. 15. SOA PDG distribution for 300 channels

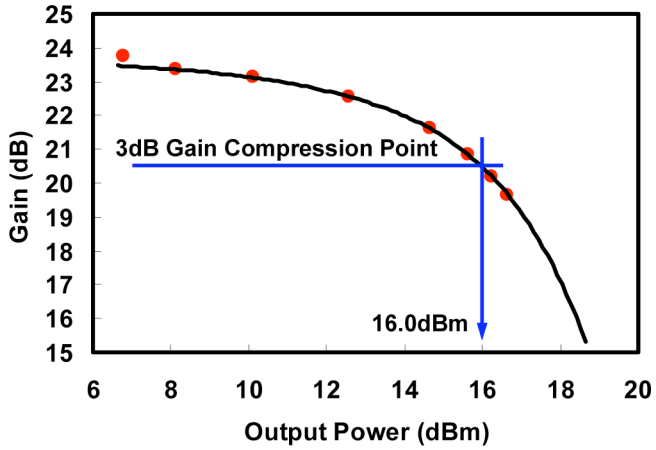

Fig. 16. Gain saturation behavior of the SOA.

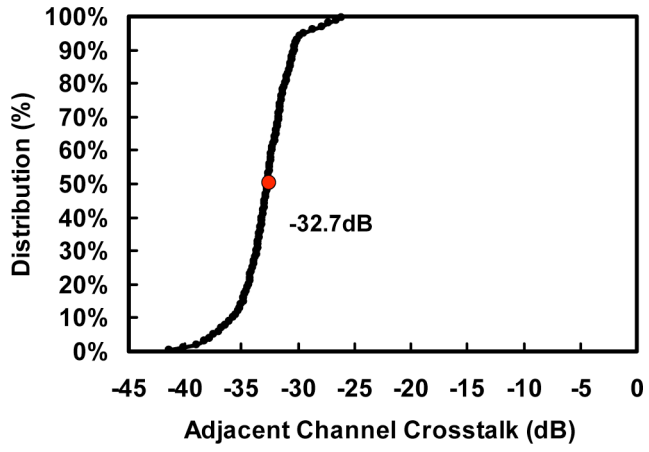

Fig. 17. For the AWG only, the adjacent channel crosstalk for 900 channels.

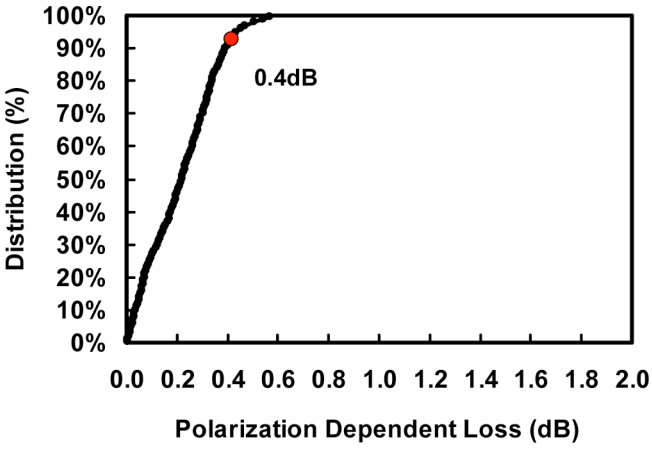

Fig. 18. For the AWG only, the PDL distribution for 900 channels.

C. AWG Performance

Figs. 17 and 18 show the performance of the AWG. This is measured independent of the SOA by using the reference channel input. In Fig. 16, the median optical adjacent channel crosstalk of the AWG is −32.7 dB. This is the worst-case optical crosstalk measured over all polarization states. The maximum optical adjacent channel crosstalk, 95% of the distribution for over 900 channels, is less than −29.5 dB. This is the performance stability of the AWG in manufacturing from PIC to PIC and wafer to wafer.

Fig. 18 shows that the PDL, for the same 900 PIC devices in Fig. 17, is less then 0.4 dB (95% point of the distribution). This measurement shows that the SOA and AWG have been individually optimized for PI operation.

D. Noise Figure Measurements

In the receiver PIC, SOA output is split into different wavelengths by an AWG and terminated with a high speed PD array. Unlike in a conventional optical amplifier, where an optical SNR (OSNR) measurement at the output of the amplifier is used to determine the noise figure (NF), we have to use the electrical method to measure the NF in the case of the SOA integrated into the receiver PIC.

In the electrical method, the NF is derived from the spectral analysis of the optical receiver photocurrent resulting from the SOA ASE noise. This method, which is considered to be more complete as it also accounts for the multipath interference noise, is covered in detail in [45] and [46]. We will only quote the relevant results here.

First, the electrical receiver needs to be calibrated. This is done by measuring the thermal noise spectrum of the PD terminated into the electrical spectrum analyzer (ESA) with the SOA turned off. This trace is the thermal noise component, $Tr_{dk}(f)$. Next, with the optical input signal, the SOA spectrum is measured using the ESA, $Tr_{\mathrm{SOA}}(f)$. The thermal noise and the shot noise (due to the average signal photocurrent I_{ave}) are subtracted from the measured SOA spectrum to obtain the corrected SOA noise spectrum, $S(f)_{\mathrm{SOA}}$. The other terms in the expression for $S(f)_{\mathrm{SOA}}$ are Z_o, the transfer function of the ESA (=50Ω), R, the responsivity of the PD, and q, the electronic charge. In addition, the measured electrical spectral traces will have to be corrected for the resolution bandwidth of the ESA

$$S(f)_{\mathrm{SOA}} = \frac{Tr_{\mathrm{SOA}}(f) - Tr_{dk}(f)}{Z_o R^2} - \frac{2q\langle I_{\mathrm{ave}}\rangle}{R^2}(\mathrm{W}^2/\mathrm{Hz}).$$

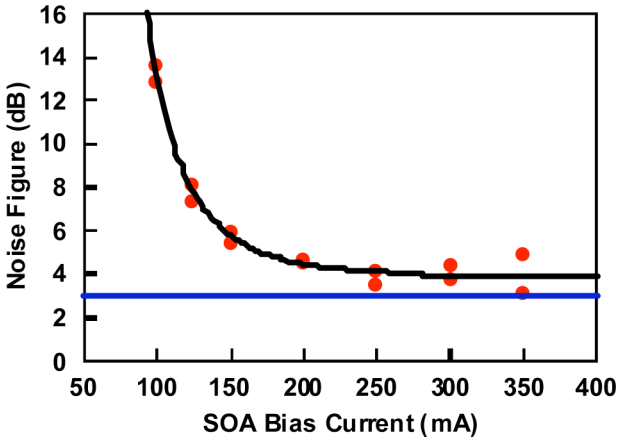

Fig. 19. NF as a function of SOA bias current.

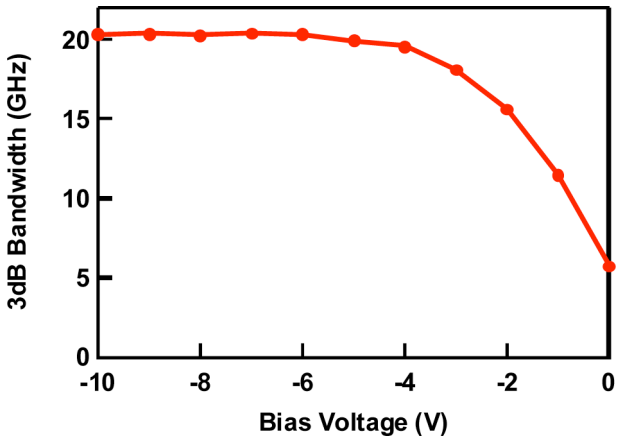

Fig. 20. Small signal bandwidth of the PD as a function of reverse bias voltage.

Based on the corrected SOA noise spectrum, the excess noise figure (NF) is given by the following equation, where h is the Planck constant, v is the optical signal frequency, G is the gain of the SOA, and P_{in} is the input optical power to the SOA:

$$\text{NF} = 10\log\left(\frac{S(f)_{\text{SOA}}}{2h\nu G^2 P_{\text{in}}}\right)(\text{dB}).$$

For the NF determination, we measured the input optical power by reverse biasing the SOA and measuring the resulting photocurrent. This allows for an accurate measurement of the input power and fiber-coupling loss. This results in the intrinsic NF of the SOA. The fiber-coupling losses add directly to this number. Fig. 19 shows the SOA NF as a function of bias current. NF decreases as the bias current increases (or as the gain increases). At high bias levels (high gains), the intrinsic NF of the SOA asymptotically tends to 4 dB. This is just 1 dB higher than the 3 dB quantum limit for optical amplifiers in the limit of high gain.

E. High Speed PD and PIC Performance

Fig. 20 shows the 3-dB electrical bandwidth of the high speed PD as a function of electrical bias. The electrical bandwidth is greater than 10 GHz at a bias of -1 V and 20 GHz at -5 V. The small signal response of the PD was measured using the Agilent 8703B lightwave component analyzer with a measurement bandwidth limit of 20 GHz.

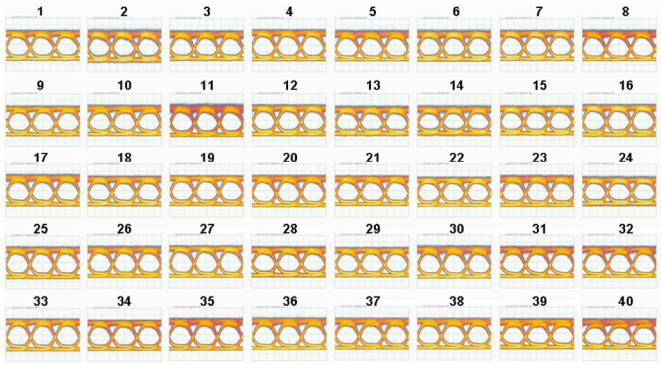

Fig. 21. Eye diagrams of the 40-channel transmitter and receiver hooked up back to back operating at 12.5 Gb/s per channel.

We connected the 40-channel transmitter [18] and the 40-channel receiver back to back and measured the eye diagrams at a data rate of 12.5 Gb/s [19]. The eye diagrams for all 40 channels, Fig. 21, are very uniform indicating the uniformity in the manufacturing process for both the RX and TX PICs. Although we have demonstrated photodiodes capable of 40 Gb/s performance [47], the AWG in the 40-channel receiver was designed for 50-GHz spacing, and hence was not designed with sufficient optical bandwidth for NRZ format data transmission at 40 Gb/s. We have also reported multichannel, impairment free operation of the SOA preamplified 10-channel $\times$ 10-Gb/s receiver in a system configuration [48].

V. Phase-Modulated Transmitter PICs

A. Phase-Modulated Systems

Phase modulation formats are recently being used to increase the spectral efficiency of WDM optical transmission systems. The benefits of phase modulation and specifically differential QPSK [(D)QPSK], however, come at the cost of increased complexity to both the transmitter and receiver architectures, especially in terms of the large number of optical functions and the corresponding number of optical elements required to realize this modulation format. Large-scale photonic integration can be used to manage this complexity by monolithically integrating multiple optical functions and multiple WDM channels onto a single chip, thus reducing the number of individual optical packages requiring fiber couplings by approximately 50–100$\times$ while simultaneously providing substantially higher reliability and reduced power consumption compared to solutions using discrete optical components [49].

B. Device Details

Fig. 22 shows the (D)QPSK transmitter PIC. Just like the 10-channel OOK PIC, it consists of 10 channels at 200-GHz channel spacing. Each channel has a tunable DFB laser and a backside power monitor. The (D)QPSK modulator of each channel uses a pair of compact InP-based Mach–Zehnder

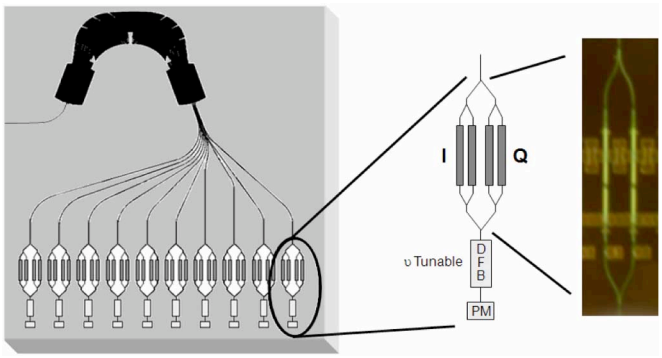

Fig. 22. Schematic diagram of the (D)QPSK transmitter PIC.

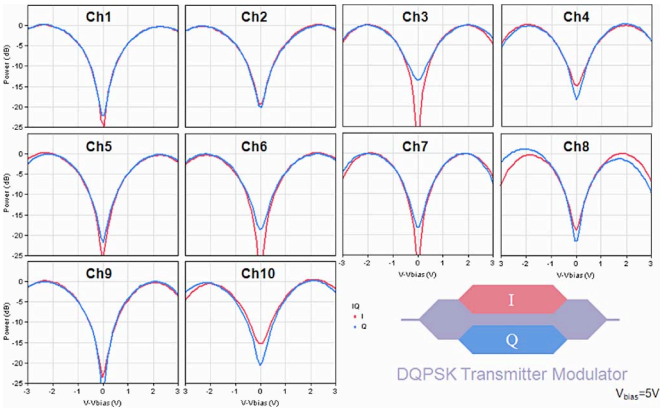

Fig. 23. MZM dc-transmission characteristics as a function of the push–pull voltage on one arm about the bias voltage for I and Q of all 10 channels.

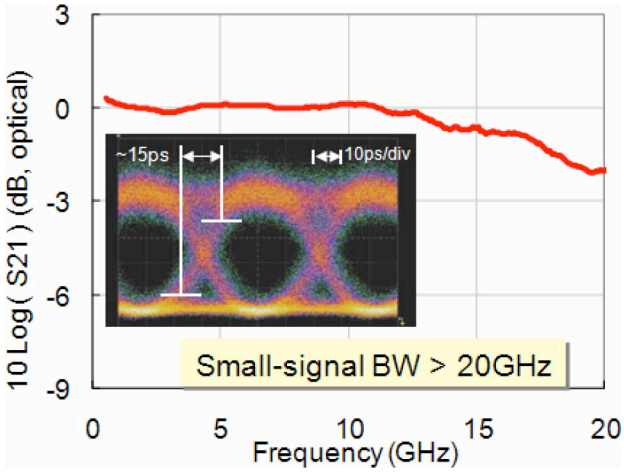

Fig. 24. Small signal bandwidth performance of the integrated MZM.

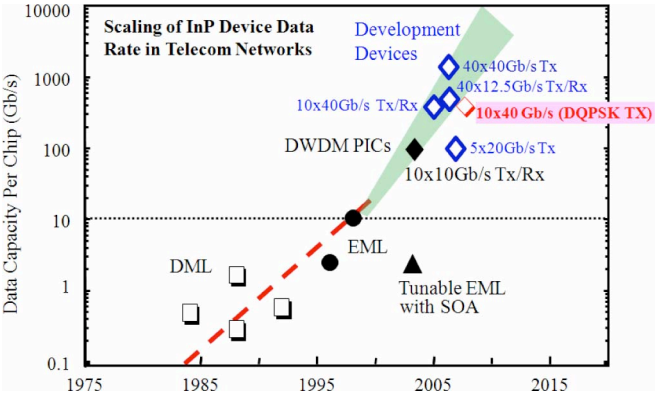

Fig. 25. Scaling of data capacity per chip for InP-based transmitters utilized in commercial telecommunications networks (in filled, black symbols). Over the last 25 years, the data capacity per chip has doubled an average of every 2.2 years.

modulators (MZMs)—one for the in-phase (I) component and one for the quadrature (Q) component—both nested within a super-MZ structure. The output waveguides of each channel are then routed into an AWG, which combines the multiple frequencies into a single output waveguide.

Fig. 23 shows the dc-transmission characteristics of the I and Q MZMs as a function of the push–pull voltage on one arm about the bias voltage for a full set of 10(I) and 10(Q) for a total of 20 MZMs. Full-swing switching voltages of 4–5 V were achieved with good uniformity across all channels of the PIC, and the extinction ratios are generally $>$20 dB.

Fig. 24 shows the RF performance of the integrated InP MZM. As a surrogate for high speed performance, the 20%–80% rise-times measured using eye diagrams from high speed NRZ modulation are about 15 ps. To measure the MZMs in the (D)QPSK mode, the modulator arm biases were adjusted to the null transmission points of each modulator and then the RF signal was applied differentially across the two arms of each MZM, which themselves were biased to be in quadrature with each other. Data and data bar signals from a 21.5 Gb/s, (2^7-1) PRBS pattern generator and a pair of broadband amplifiers were fed to the I and Q MZMs. An electrical delay was applied to data bar to decorrelate the two-bit sequences, and electrical phase adjusters were used to bit-align I and Q signals. Clear and open eyes were recovered for both data streams using a receiver consisting of a delay line interferometer and a commercial balanced receiver. The data streams combine to yield a 43-Gb/s total transmission rate per channel [49].

VI. Commercial Large-Scale PICs

Although PICs of increasing levels of complexity and sophistication have been demonstrated over the years, by many groups, most of these have not been commercialized successfully. Our 10-channel, 10 Gb/s per channel PIC [17] that was first deployed in late 2004, is to date the only reported successful example of a PIC carrying live traffic in the field. Fig. 25 shows how the data-carrying capacity of monolithically integrated PICs have evolved over time. Until our deployment of a 100-Gb/s PIC, the highest data rate for a commercial PIC was at 10 Gb/s for the preceding 10 years. Experimental devices with total aggregate capacity up to 1 Tbit/s have been demonstrated to date (shown on the same chart as blue diamond). To successfully commercialize a PIC, a good design has to go hand in hand with good manufacturing and reliability infrastructure. Going forward, photonic integration is essential to keep up with ever increasing Internet data traffic, and the need for smaller equipment footprint and lower power consumption.

ACKNOWLEDGMENT

The authors would like to thank the very talented technical team at Infinera for their role in commercializing the first LS-PIC and help with the development work described here. They would also like to thank Prof. M. Smit of Technische Universiteit Eindhoven for working with one of the authors (RN) on the PIC benchmarking exercise.

REFERENCES

[1] R. Nagarajan and M. Smit, "Photonic integration," *IEEE LEOS Newslett.*, vol. 21, no. 3, pp. 4–10, Jun. 2007.

[2] S. E. Miller, "Integrated optics: An introduction," *Bell Sys. Tech. J.*, vol. 48, pp. 2059–2069, Sep. 1969.

[3] I. Hayashi, M. B. Panish, P. W. Foy, and S. Sumski, "Junction lasers which operate continuously at room temperature," *Appl. Phys. Lett.*, vol. 17, pp. 109–111, Aug. 1970.

[4] J. Shibata, I. Nakao, Y. Sasai, S. Kimura, N. Hase, and H. Serizawa, "Monolithic integration of an InGaAsP/InP laser diode with heterojunction bipolar transistors," *Appl. Phys. Lett.*, vol. 45, pp. 191–193, Aug. 1984.

[5] O. Wada, T. Sakurai, and T. Nakagami, "Recent progress in optoelectronic integrated circuits (OEICs)," *IEEE J. Quantum Electron.*, vol. QE-22, no. 6, pp. 805–821, Jun. 1986.

[6] T. L. Koch and U. Koren, "Semiconductor photonic integrated circuits," *IEEE J. Quantum Electron.*, vol. QE-27, no. 3, pp. 641–653, Mar. 1991.

[7] M. Zirngibl, C. H. Joyner, and L. W. Stultz, "WDM receiver by monolithic integration of an optical preamplifier, waveguide grating router and photodiode array," *Electron Lett.*, vol. 31, pp. 581–582, Mar. 1995.

[8] C. A. M. Steenbergen, C. Van Dam, A. Looijen, C. G. P. Herben, M. De Kok, M. K. Smit, J. W. Pedersen, I. Moerman, R. G. F. Baets, and B. H. Verbeek, "Compact low loss 8 × 10 GHz polarisation independent WDM receiver," in *Proc. Eur. Conf. Opt. Commun.*, Sep. 1996, vol. 1, pp. 129–132.

[9] C. G. P. Herben, D. H. P. Maat, X. J. M. Leijtens, M. R. Leys, Y. S. Oei, and M. K. Smit, "Polarization independent dilated WDM cross-connect on InP," *Photon. Technol. Lett.*, vol. 11, pp. 1599–1601, Dec. 1999.

[10] L. A. Coldren, "Monolithic tunable diode lasers," *J. Sel. Topics Quantum Electron.*, vol. 6, pp. 988–999, Nov. 2000.

[11] Y. Yoshikuni, "Semiconductor arrayed waveguide gratings for photonic integrated devices," *J. Sel. Topics Quantum Electron.*, vol. 8, pp. 1102–1114, Dec. 2002.

[12] N. Kikuchi, Y. Shibata, H. Okamoto, Y. Kawaguchi, S. Oku, H. Ishii, Y. Yoshikuni, and Y. Tohmori, "Monolithically integrated 64-channel WDM channel selector on InP substrate," in *Proc. Eur. Conf. Opt Commun.*, Sep. 2001, vol. 1, pp. 4–5.

[13] Y. Suzaki, K. Asaka, Y. Kawaguchi, S. Oku, Y. Noguchi, S. Kondo, R. Iga, and H. Okamoto, "Multi-channel modulation in a DWDM monolithic photonic integrated circuit," in *Proc. Int. Conf. Indium Phosphide Related Mater.*, May 2002, pp. 681–683.

[14] M. L. Mašanović, V. Lal, J. S. Barton, E. J. Skogen, L. A. Coldren, and D. J. Blumenthal, "Monolithically integrated Mach-Zehnder interferometer wavelength converter and widely tunable laser in InP," *Photon. Technol. Lett.*, vol. 15, pp. 1117–1119, Aug. 2003.

[15] V. I. Tolstikhin, A. Densmore, Y. Logvin, K. Pimenov, F. Wu, and S. Laframboise, "44-channel optical power monitor based on an echelle grating demultiplexer and a waveguide photodetector array monolithically integrated on an InP substrate," presented at Opt. Fiber Commun. Conf., Atlanta, GA, Mar. 2003, Paper PD37-1.

[16] ASIP/Three-Five Photonics. (2004, May). [Online]. Available: www.rle.mit.edu/cips/conference04/Pennings_ASIP.pdf

[17] R. Nagarajan, C. Joyner, R. Schneider, Jr., J. Bostak, T. Butrie, A. Dentai, V. Dominic, P. Evans, M. Kato, M. Kauffman, D. Lambert, S. Mathis, A. Mathur, R. Miles, M. Mitchell, M. Missey, S. Murthy, A. Nilsson, F. Peters, S. Pennypacker, J. Pleumeekers, R. Salvatore, R. Schlenker, R. Taylor, H. Tsai, M. Van Leeuwen, J. Webjorn, M. Ziari, D. Perkins, J. Singh, S. Grubb, M. Reffle, D. Mehuys, F. Kish, and D. Welch, "Large-scale photonic integrated circuits," *IEEE J. Sel. Top. Quantum Electron.*, vol. 11, no. 1, pp. 50–65, Jan./Feb. 2005.

[18] R. Nagarajan, M. Kato, J. Pleumeekers, P. Evans, D. Lambert, A. Chen, V. Dominic, A. Mathur, P. Chavarkar, M. Missey, A. Dentai, S. Hurtt, J. Baeck, R. Muthiah, S. Murthy, R. Salvatore, S. Grubb, C. Joyner, J. Rossi, R. Schneider, M. Ziari, F. Kish, and D. Welch, "Single-chip 40-channel InP transmitter photonic integrated circuit capable of aggregate data rate of 1.6 Tbit/s," *Electron. Lett.*, vol. 42, no. 13, pp. 771–773, May 2006.

[19] M. Kato, R. Nagarajan, J. Pleumeekers, P. Evans, A. Chen, A. Mathur, A. Dentai, S. Hurtt, D. Lambert, P. Chavarkar, M. Missey, J. Baeck, R. Muthiah, S. Murthy, R. Salvatore, C. Joyner, J. Rossi, R. Schneider, M. Ziari, F. Kish, and D. Welch, "40-channel transmitter and receiver photonic integrated circuits operating at per channel data rate 12.5 Gbit/s," *Electron. Lett.*, vol. 43, no. 8, pp. 468–469, Apr. 2007.

[20] R. Nagarajan, M. Kato, S. Hurtt, A. Dentai, J. Pleumeekers, P. Evans, M. Missey, R. Muthiah, A. Chen, D. Lambert, P. Chavarkar, A. Mathur, J. Bäck, S. Murthy, R. Salvatore, C. Joyner, J. Rossi, R. Schneider, M. Ziari, F. Kish, and D. Welch, "Monolithic, 10 and 40 channel InP receiver photonic integrated circuits with on-chip amplification," presented at Opt. Fiber Commun. Conf., Anaheim, CA, Mar. 2007, Paper PDP32.

[21] S. C. Nicholes, M. L. Mašanović, B. Jevremović, E. Lively, L. A. Coldren, and D. J. Blumenthal, "The world's first InP 8×8 monolithic tunable optical router (MOTOR) operating at 40 Gbps line rate per port," presented at Opt. Fiber Commun. Conf., San Diego, CA, Mar. 2009, Paper PDPB1.

[22] C. Joyner, J. Pleumeekers, A. Mathur, P. Evans, D. Lambert, S. Murthy, S. Mathis, F. Peters, J. Baeck, M. Missey, A. Dentai, R. Salvatore, R. Schneider, Jr., M. Ziari, M. Kato, R. Nagarajan, J. Bostak, T. Butrie, V. Dominic, M. Kauffman, R. Miles, M. Mitchell, A. Nilsson, S. Pennypacker, R. Schlenker, R. Taylor, H. Tsai, M. Van Leeuwen, J. Webjorn, D. Perkins, J. Singh, S. Grubb, M. Reffle, D. Mehuys, F. Kish, and D. Welch, "Large-scale DWDM photonic integrated circuits: A manufacturable and scalable integration platform," presented at the LEOS Annu. Meeting, Sydney, Australia, Oct. 2005, Paper TuU2.

[23] F. Kish, D. Welch, J. Pleumeekers, A. Mathur, P. Evans, R. Muthiah, S. Murthy, M. Kauffman, P. Freeman, R. Schneider, Jr., M. Ziari, C. Joyner, J. Bostak, T. Butrie, A. Dentai, V. Dominic, S. Hurtt, M. Kato, D. Lambert, R. Miles, M. Mitchell, M. Missey, R. Nagarajan, F. Peters, S. Pennypacker, R. Salvatore, R. Schlenker, R. Taylor, H. Tsai, M. Van Leeuwen, J. Webjorn, S. Grubb, M. Reffle, D. Mehuys, D. Perkins, and J. Singh, "Volume manufacturing and deployment of large-scale photonic integrated circuits," presented at the Opt. Fiber Commun. Conf. (OFC), Anaheim, USA, Mar. 2006, Paper OWL1.

[24] D. Welch, C. Joyner, D. Lambert, P. Evans, and M. Raburn, "III-V photonic integrated circuits and their impact on optical network architectures," in *Optical Fiber Telecommunications VA*, I. Kaminow, T Li, and A. Willner, Eds. Massachusetts: Academic, 2008, pp. 343–379.

[25] E. Skogen, J. Barton, S. Denbaars, and L. Coldren, "A quantum-well intermixing process for wavelength-agile photonic integrated circuits," *IEEE J. Sel. Topics Quantum Electron.*, vol. 8, no. 4, pp. 863–869, Jul./Aug. 2002.

[26] V. I. Tolstikhin, R. Moore, K. Pimenov, Y. Logvin, F. Wu, and C. D. Watson, "One-step growth optical transceiver PIC in InP," presented at the Eur. Conf. Opt. Commun. (ECOC), Vienna, Austria, Sep. 2009, Paper 8.6.2.

[27] R. Broeke, J. Cao, C. Ji, S. Seo, Y. Du, N. Fontaine, J. Baek, J. Yan, F. Soares, F. Olsson, S. Lourdudoss, A. Pham, M. Shearn, A. Scherer, and S. Yoo, "Optical-CDMA in InP," *IEEE J. Sel. Topics Quantum Electron.*, vol. 13, no. 5, pp. 1497–1507, Sep./Oct. 2007.

[28] S. Murthy, M. Kato, R. Nagarajan, M. Missey, V. Dominic, V. Lal, B. Taylor, J. Pleumeekers, J. Zhang, P. Evans, M. Ziari, R. Muthiah, R. Salvatore, H. Tsai, A. Nilson, D. Pavinski , P. Studenkov, S. Agashe, A. Dentai, D. Lambert, J. Bostak, J. Stewart, C. Joyner, J. Rossi, R. Schneider, M. Reffle, F. Kish, and D. Welch, "Large-scale photonic integrated circuit transmitters with monolithically integrated semiconductor optical amplifiers," presented at Opt. Fiber Commun. Conf., San Diego, CA, Mar. 2008, Paper OTuN1.

[29] M. Newkirk, B. Miller, U. Koren, M. Young, M. Chien, R. Jopson, and C. Burrus, "1.5 μm multiquantum-well semiconductor optical amplifier with tensile and compressively strained wells for polarization-independent gain," *IEEE Photon. Technol. Lett.*, vol. 4, no. 4, pp. 406–408, Apr. 1993.

[30] P. Thijs, L. Tiemeijer, J. Binsma, and T. Dongen, "Progress in long-wavelength strained-layer InGaAs(P) quantum-well semiconductor lasers and amplifiers," *IEEE J. Quantum Electron.*, vol. 30, no. 2, pp. 477–499, Feb. 1994.

[31] K. Magari, M. Okamoto, Y. Suzuki, K. Sato, Y. Noguchi, and O. Mikami, "Ploarization-insensitive optical amplifier with tensile-strained-barrier MQW structure," *IEEE J. Quantum Electron.*, vol. 30, no. 3, pp. 695–702, Mar. 1994.

[32] P. Thijs, L. Tiemeijer, J. Binsma, and T. Dongen, "Strained-layer InGaAs(P) quantum well semiconductor lasers and semiconductor laser amplifiers," *Philips J. Res.*, vol. 49, pp. 187–224, Mar. 1995.
[33] J.-Y. Emery, T. Ducellier, M. Bachmann, P. Doussière, F. Pommereau, R. Ngo, F. Gaborit, L. Goldstein, G. Laube, and J. Barrau, "High performance 1.55 μm polarization-independent semiconductor optical amplifier based on low-tensile-strained bulk GaInAsP," *Electron. Lett.*, vol. 33, no. 12, pp. 1083–1084, Jun. 1997.
[34] T. Kakitsuka, Y. Shibata, M. Itoh, Y. Kadota, Y. Tohmori, and Y. Yoshikuni, "Influence of buried structure on polarization sensitivity in strained bulk semiconductor optical amplifiers," *IEEE J. Quantum Electron.*, vol. 38, no. 1, pp. 85–92, Jan. 2002.
[35] K. Dreyer, C. Joyner, J. Pleumeekers, C. Burrus, A. Dentai, B. Miller, S. Shunk, P. Sciortino, S. Chandrasekhar, L. Buhl, F. Storz, and M. Farwell, "High-gain mode-adapted semiconductor optical amplifier with 12.4-dBm saturation output power at 1550 nm," *IEEE J. Lightwave Technol.*, vol. 20, no. 4, pp. 718–721, Apr. 2002.
[36] P. Koonath, S. Kim, W.-J. Cho, and A. Gopinath, "Polarization insensitive quantum-well semiconductor optical amplifiers," *IEEE J. Quantum Electron.*, vol. 38, no. 9, pp. 1282–1290, Sep. 2002.
[37] K. Morito, M. Ekawa, T. Watanabe, and Y. Kotaki, "High-output-power polarization-insensitive semiconductor optical amplifier," *IEEE J. Lightwave Technol.*, vol. 21, no. 1, pp. 176–181, Jan. 2003.
[38] C. Michie, A. Kelly, J. McGeough, I. Armstrong, I. Andonovic, and C. Tombling, "Polarization-insensitive SOAs using strained bulk active regions," *IEEE J. Lightwave Technol.*, vol. 24, no. 11, pp. 3920–3927, Nov. 2006.
[39] M. Smit and C. van Dam, "PHASAR-based WDM-devices: Principles, design and applications," *IEEE J. Sel. Topics Quantum Electron.*, vol. 2, no. 2, pp. 236–250, Jun. 1996.
[40] K. Okamoto, "Recent progress of integrated optics planar lightwave circuits," *Opt. Quantum Electron.*, vol. 31, pp. 107–129, 1999.
[41] M. Zirngibl, C. H. Joyner, and P. C. Chou, "Polarisation compensated waveguide grating router on InP," *Electron. Lett.*, vol. 31, no. 1, pp. 1662–1664, Sep. 1995.
[42] J. den Besten, M. Dessens, C. Herben, X. Leijtens, F. Groen, M. Leys, and M. Smit, "Low-loss, compact, and polarization independent PHASAR demultiplexer fabricated by using a double-etch process," *IEEE Photon. Technol. Lett.*, vol. 14, no. 1, pp. 62–64, Jan. 2002.
[43] A. Sugita, A. Kaneko, K. Okamoto, M. Itoh, A. Himeno, and Y. Ohmori, "Very low insertion loss arrayed-waveguide grating with vertically tapered waveguides," *IEEE Photon. Technol. Lett.*, vol. 12, no. 9, pp. 1180–1182, Sep. 2000.
[44] *BeamPROP*$^{\mathrm{TM}}$, RSoft Design Group, Ossining, NY.
[45] D. Baney, "Characterization of Erbium-doped fiber amplifier," in *Fiber Optic Test and Measurement*, D. Derickson, Ed. Englewood Cliffs, NJ: Prentice-Hall, 1997, pp. 519–595.
[46] D. Baney, P. Gallion, and R. Tucker, "Theory and measurement techniques for the noise figure of optical amplifiers," *Opt. Fiber Technol.*, vol. 6, pp. 122–154, 2000.
[47] R. Nagarajan, M. Kato, V. Dominic, C. Joyner, R. Schneider, Jr., A. Dentai, T. Desikan, P. Evans, M. Kauffman, D. Lambert, S. Mathis, A. Mathur, M. Mitchell, M. Missey, S. Murthy, A. Nilsson, F. Peters, J. Pleumeekers, R. Salvatore, R. Taylor, M. Van Leeuwen, J. Webjorn, M. Ziari, S. Grubb, D. Perkins, M. Reffle, D. Mehuys, F. Kish, and D. Welch, "400 Gb/s (10-channel $\times$ 40Gb/s) DWDM photonic integrated circuits," *Electron. Lett.*, vol. 41, pp. 347–349, Mar. 2005.
[48] R. Nagarajan, M. Kato, V. Dominic, S. Hurtt, A. Dentai, J. Pleumeekers, P. Evans, M. Missey, R. Muthiah, A. Chen, D. Lambert, P. Chavarkar, A. Mathur, J. Bäck, S. Murthy, R. Salvatore, H. Tsai, D. Pavinski, C. Joyner, J. Rossi, R. Schneider, M. Ziari, M. Reffle, D. Mehuys, F. Kish, and D. Welch, "Multi-channel operation of a receiver photonic integrated circuit with an integrated semiconductor optical amplifier," presented at the Eur. Conf. Opt. Commun. (ECOC), Berlin, Germany, Sep. 2007, Paper 05.5.5.
[49] S. Corzine, P. Evans, M. Kato, G. He, M. Fisher, M. Raburn, A. Dentai, I. Lyubomirsky, A. Nilsson, J. Rahn, R. Nagarajan, C. Tsai, J. Stewart, D. Christini, M. Missey, V. Lal, H. Dinh, A. Chen, J. Thomson, W. Williams, P. Chavarkar, S. Nguyen, D. Lambert, S. Agashe, J. Rossi, P. Liu, J. Webjorn, T. Butrie, M. Reffle, R. Schneider, M. Ziari, C. Joyner, S. Grubb, F. Kish, and D. Welch, "10-Channel $\times$ 40 Gb/s per channel DQPSK monolithically integrated InP-based transmitter PIC," presented at Opt. Fiber Commun. Conf., San Diego, CA, Feb. 2008, Paper PDP18.

Radhakrishnan Nagarajan (S'85–M'86–SM'97–F'08) obtained the B.Eng. (first class Hons.) in electrical engineering from the National University of Singapore, Singapore, in 1986, the M.Eng. degree in electronic engineering from the University of Tokyo, Tokyo, Japan, in 1989, and the Ph.D. degree in electrical engineering from the University of California, Santa Barbara, in 1992.

He was a Research Faculty with the University of California, Santa Barbara. In 1995, he joined SDL. He was a Senior Manager with the Advanced Technology Group, JDS Uniphase, Milpitas, CA, where he was engaged in next generation high-speed optical components. Since 2001, he has been with Infinera Corporation, Sunnyvale, CA, where he is currently a Fellow, Optical Component Technology and he has been engaged on photonic integration and related technologies. He was as a Guest Editor of the *Optical & Quantum Electronics* and *Applied Optics* journals. He has authored or coauthored more than 150 publications in journals and conferences, and three book chapters mainly in the area of high-speed optical components. He holds 38 U.S. patents.

Dr. Nagarajan is a Fellow of the Optical Society of America and a Fellow of the Institution of Engineering and Technology. He received the Photonics Circle of Excellence Award in 2000 for the development of the new generation 980 nm pump module. He was the recipient of the 2006 IEEE Laser and Electrooptics Society Aron Kressel Award for his contributions to commercializing large-scale photonic integrated circuits.

Masaki Kato (M'97) received the B.S., M.S., and Ph.D. degrees in electronic engineering from the University of Tokyo, Tokyo, Japan in 1994, 1996, and 1999, respectively.

In 1999, he was a Research Associate with the Department of Electrical Engineering, University of Tokyo, where he was involved in studying semiconductor optical devices and their application for wavelength conversion/all-optical switching. In 2002, he joined Infinera Corporation, Sunnyvale, CA, as a member of Technical Staff, where he has been engaged in the development of large-scale photonic integrated circuits. He has authored or coauthored more than 50 journals and conferences.

Dr. Kato is a member of Japanese Society of Applied Physics.

Jacco Pleumeekers received the M.Sc. and Ph.D. degrees in electrical engineering from the Delft University of Technology, Delft, The Netherlands, in 1992 and 1997, respectively.

From 1992 to 1996, he was with France Telecom Research Laboratory, Lannion, France, where he was engaged in Ph.D. research on numerical simulations for optoelectronic devices. From 1996 to 1999, he was a Postdoctoral Fellow with the Ecole Polytechnique Federale de Lausanne, Switzerland, where he was engaged in both theoretical and experimental research into semiconductor optical amplifiers. From 1999 to 2001, he was a member of Technical Staff with Lucent Technologies, Bell Laboratories, Holmdel, NJ, where he was involved in a variety of projects in the field of all-optical signal processing with integrated optoelectronic devices. Since 2001, he has been with Infinera Corporation, Sunnyvale, CA, where he is currently managing a Product Engineering Team responsible for photonic device integration. He has authored or coauthored more than 50 papers and conference contributions and holds two patents related to optical devices.

Peter Evans was born in St. Louis, MO, in 1972. He received the B.S., M.S., and Ph.D. degrees in electrical engineering from the University of Illinois, Urbana-Champaign, in 1994, 1996, and 1998, respectively.

His Ph.D. work on coinventing buried-tunnel-contact vertical cavity surface emitting lasers (VCSELs) was in part supported by an National Science Foundation Fellowship, 1995–1998. He then developed processes for implant and oxide VCSEL fabrication at Hewlett-Packard/Agilent until 1999. From 1999 to 2002, he was with Genoa Corporation, Fremont, CA, where he was involved in the developement of epitaxial materials, processes and devices, including long-wavelength VCSELs and linear optical amplifiers for telecomm applications. He is currently a photonic integrated circuit Product Development Engineer with Infinera Corporation, Sunnyvale, CA, where he is also involved in fabrication processes, reliability, and device integration, since 2002. He is the author or coauthor of the Optical Fiber Telecommunications Components and Subsystems (Academic Press, 5th ed., 2008).

Scott Corzine was born in Nashville, TN, in 1963. He received the B.S., M.S., and Ph.D. degrees from the Department of Electrical and Computer Engineering, University of California, Santa Barbara.

He was involved in the theoretical and experimental investigation of vertical-cavity surface-emitting lasers. For ten years, he was with Agilent Laboratories, Palo Alto, CA, where he was engaged in working on the design and fabrication of various optoelectronic devices. He is currently with Infinera Corporation, Sunnyvale, CA, where he is engaged in current and next-generation photonic integrated circuits. He has couthored a graduate-level textbook on semiconductor lasers and has also contributed a chapter to a book on quantum-well lasers.

Sheila Hurtt, photograph and biography not available at the time of publication.

Andrew Dentai (M'72–SM'82–F'93) received his B.Sc. degree from the University of Veszprem, Veszprém, Hungary, in 1966, and the M.S. and Ph.D. degrees in ceramic science from Rutgers University, Newark, NJ, in 1972 and 1974, respectively.

He joined Bell Laboratories, Murray Hill, NJ, in 1968 and further rejoined in 1974, where he was engaged in epitaxial crystal growth, first employing LPE, and later switching to MOVPE. He was involved in material development for long wavelength light-emmiting diodes (LEDs), separate absorption and graded multiplication Avalanche photodectectors, LED-pumped Nd: YAG fiber lasers, tunable Y-branch lasers, long wavelength photodiodes, high speed photodiodes, InP-based single heterojunction bipolar transistor (HBT) and double HBT, and optoelectronic integrated circuit receivers based on HBTs among other devices. He was named a Distinguished Member of Technical Staff of Bell Laboratories in 1987. Since 2001, he has been with the Technical Staff of Infinera's Epi operations, Infinera Corporation, Sunnyvale, CA, where he has been enggaed in working on materials for photonic integrated circuits. He has more than 300 publications and talks, and holds 30 patents spanning 31 years at Bell Laboratories and 6 years at Infinera.

Sanjeev Murthy received the B.Tech. degree in electronics and communication engineering from the Indian Institute of Technology, Chennai, India, in 1994, and the M.S. and Ph.D degrees in electrical engineering from the University of California, Los Angeles, in 1999 and 2004, respectively.

He was involved in optical and electrical designs for high-speed, high-power, and high-responsivity distributed photodetectors. Since 2002, he has been with Infinera Corporation, Sunnyvale, CA, where he has been engaged on several aspects of photonic integrated circuit design for transmitter and receiver applications.

Mark Missey received the B.S. degree in physics from St. Louis University, St. Louis, MO, in 1994, the M.S. and Ph.D. degrees in electrooptics from the University of Dayton, Dayton, OH, in 1996 and 1999, respectively.

He was a Research Scientist in the Technology Development Group with SDL/JDS Uniphase, San Jose, CA, where he was engaged in investigating applications for several emerging technologies, including microelectromechanical system, planar waveguide circuits, and Raman amplification. In 2001, he joined Infinera Corporation, Sunnyvale, CA, as a member of Technical Staff, where he has been engaged in providing key design and test contributions to the company's first-generation large-scale photonic integrated circuits and currently oversees the test development for next-generation photonic integrated circuits.

Ranjani Muthiah (M'05) received the B.Tech. degree in metallurgical engineering from the Institute of Technology, Banaras Hindu University, Varanasi, India, in 1992, and the Ph.D. degree in materials science and engineering from University of Pennsylvania, Philadelphia, in 1997.

From 1997 to 2002, she was a member of Technical Staff with the Optoelectronics Division, Lucent Technologies/Agere Systems, Breinigsville, PA. She worked as a Process Engineer until 2000 and was instrumental in improving the metallization process for lasers and detectors. From 2000 to 2002, she was involved in a number of product yield improvement activities. In 2003, she was a Reliability Engineer with Infinera Corporation, Sunnyvale, CA, where she is currently a Reliability Engineering Manager with the Optical Integrated Components Group. She has authored or coauthored more than 20 journal publications and conference presentations in the fields of materials science, semiconductor processing, and optics.

Randal A. Salvatore (S'91–M'96) received the B.S.E. degree (*summa cum laude*) from the University of Michigan, Ann Arbor, in 1990, and the M.S. and Ph.D. degrees in electrical engineering from the California Institute of Technology, Pasadena, in 1991 and 1996.

From 1991 to 1995, he was engaged in studying femtosecond and high-repetition-rate sources and demonstrated the first adjustable chirp, passively modelocked semiconductor laser. From 1996 to 1997, he was a Visiting Researcher with the University of California, Santa Barbara, where he was engaged on noise properties in semiconductor lasers and on wavelength conversion. In 1997, he was a Principal Engineer with Lasertron, Inc., Bedford, MA, where he was engaged on high-power pump lasers, distributed feedback lasers, and modulators. Since 2002, he has been with Infinera Corporation, Sunnyvale, CA. He has authored more than 25 journal papers and conference presentations, and holds six patents.

Dr. Salvatore is a member of the Optical Society of America, Phi Beta Kappa, and Tau Beta Pi.

Charles Joyner was born in Decatur Georgia, in 1953. He received the Bachelor's degree in chemistry from Furman University, Greenville, SC, in 1975, the Master's and PhD. degrees in physical chemistry from Harvard University, Cambridge, MA, in 1978 and 1981, respectively.

In 1981, he was a member of Technical Staff with AT&T Bell Laboratories, Murray Hill, NJ. He was enggaed in design and fabrication of InP-based integrated photonic devices for telecommunications. In August 2000, he was a Technical Manager in charge of semiconductor photonics with Lucent Bell Laboratories. In July 2001, he joined Infinera Corporation, Sunnyvale, CA, as Director of Device Development. He has authored or coauthored more than 100 papers and is a coauthor of Optical Telecommunications III and V (1997 and 2008). He holds 39 patents.

Dr. Joyner is a Senior Member of IEEE/Laser and Electrooptics Society (LEOS) and a Fellow of the Optical Society of America in 2003. He was the receipient of the Aron Kressel LEOS Award in 2006 for important contributions to optoelectronic device technology, which has found its way into widespread usage.

Richard Schneider, Jr. was born in Akron, OH, in 1962. He received the B. S. degree in physical metallurgy from Washington State University, Pullman, WA, in 1984, and the Ph.D. degree in materials science and engineering from Northwestern University, Evanston, IL, in 1989.

From 1989 to 1995, he was a Senior Member of Technical Staff with Sandia National Laboratories, Albuquerque, NM, where he was invovled in working on vertical-cavity surface-emitting laser (VCSEL) technology, including the first AlGaInP-based visible VCSELs, development of metalorganic vapor phase epitaxy for VCSEL production, and demonstration of high-efficiency VCSELs using oxide confinement. In 1995, he was with Hewlett-Packard Laboratories (later Agilent Laboratories), Palo Alto, CA, where he was engaged in VCSEL device development and transfer to the manufacturing division. Later, he was responsible for developing epitaxy processes for GaN-based visible LEDs and continuous-wave violet laser diodes, and then managed the Advanced GaN Optoelectronics R&D group. In 2000, he was with the Fiber Optics Division, Agilent Laboratories, where he was engaged in managing VCSEL epitaxy and device manufacturing and R&D teams. Since 2001, he was with Infinera Corporation, Sunnyvale, CA, where he has been involved in the development of epitaxial materials processes for Infinera's photonic integrated circuits. He is currently enggaed in managing epitaxial materials technology and integration engineering manufacturing and development activities. He has been an Associate Editor for the *Journal of Electronic Materials* since 1999.

Dr. Schneider is a Fellow of the Optical Society of America.

Mehrdad Ziari (M'95) received the Bachelor's (*suma cum laude*) degree (Hons.), and the M.Sc. and Ph.D. degrees in electrical engineering from the University of Southern California (USC), Los Angeles, CA, in 1986, 1987, and 1992, respectively.

He was a Postdoctoral Researcher at the USC Center for Photonic Technology and was engaged in research in nonlinear optics and organic polymer waveguide devices. In 1995, he was with SDL, Inc., where he was engaed on various laser diode and optical component technologies,managed InP R&D activities, and also led to the development of Raman pump laser diode products. Since 2002, he has been with Infinera Corporation, Sunnyvale, CA, where he is currently the Director of device development and engineering. He has authored or coauthored more than 75 papers, two book chapters, and holds more than 30 patents.

Fred Kish (M'93–SM'01) received the B.S., M.S., and Ph.D. degrees in electrical engineering form the University of Illinois at Urbana-Champaign, in 1988, 1989, and 1992, respectively.

He is currently a Vice President of photonic integrated circuit development and manufacturing with Infinera Corporation, Sunnyvale, CA. He was the Manager of R&D and Manufacturing Department with Agilent Technologies, where he was engaged in the III–V optoelectronic component organization for Agilent's fiber-optics business. He held several positions in senior management at Agilent/Hewlett-Packard, where he was responsible for the development of visible light emitter technology and was one of the core Inventors of transparent-substrate AlInGaP light-emitting diodes. He has coauthored 50 peer-reviewed publications and holds more than 30 patents in the area of III-V optoelectronic devices.

Dr. Kish has been awarded the 1996 Adolph Lomb Award from the Optical Society of America, the International Symposium on Compound Semiconductors 1997 Young Scientist Award, the 1999 IEEE Laser and Electrooptics Society Engineering Achievement Award, and the 2004 IEEE David Sarnoff Award.

David Welch (M'81–SM'90–F'08) received the B.S. degree in electrical engineering from the University of Delaware, Newark, 1981, and the Ph.D. degree in electrical engineering from Cornell University, Ithaca, NY, 1984.

In 2001, he founded Infinera Corporation, Sunnyvale, CA, an optical networking company, where he is currently the Chief Strategy and Marketing Officer. He was the Chief Technology Office and the Vice President of Corporate Development of SDL and JDS Uniphase, where he was engaged in technology and acquisition strategies that culminated in the $41B acquisition of SDL by JDS Uniphase. He has authored or coauthored more than 250 articles and holds more than 100 patents in optical components and systems.

Dr. Welch is an Optical Society of America (OSA) Fellow. He was the recipient of the Adolph Lomb Award (1992) from OSA, the Engineering Achievement Award from Laser and Electrooptics Society (1998), and the Fraunhofer Award (1999) from OSA. He was on the board of Directors of OSA.